ACS OMEGA

http://pubs.acs.org/journal/acsodf

Article

AlInGaAs MQW Transceiver with Electro-optic Modulation Characteristics for Free-Space Optical Communication and Sensing

Xin Li,* Xu Wang, Yun Li, Feifei Qin, Yan Jiang, Linning Wang, and Yongjin Wang*

Cite This: *ACS Omega* 2021, 6, 23614−23620

Read Online

ACCESS | Metrics & More | Article Recommendations

ABSTRACT: Integrated transceivers with electro-optic modulation characteristics are valuable for free-space optical communications and sensing. We propose an AlInGaAs multiple quantum well (MQW) transceiver with electro-optic modulation characteristics over a broad spectral range. Two identical AlInGaAs MQW diodes on a single wafer are used to transmit and receive optical signals and provide obvious electro-optic modulation for broad-spectrum light. The photocurrent modulation ratio reaches 13.9 and 11.3 for white light and 1550 nm infrared light, respectively, with varying bias voltages. The transceiver can identify environmental changes and forward electrical signals with different frequencies in the form of superimposed optical signals.

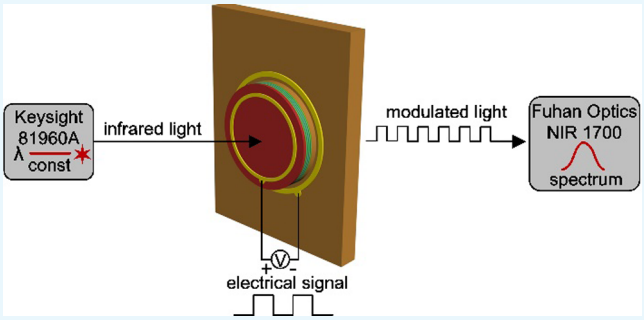

INTRODUCTION

Transceiver modules for optical communication applications have been used widely in industry.[1−3] A transceiver module is composed of independent transmitters, receivers, functional circuits, optical interfaces, and other structural components.[4−6] To enable miniaturization of optical communication equipment, it is necessary to develop integrated transceivers.[7,8] The study of integrated transceivers is also driven by the various applications of these devices, which include sensing, the Internet of Things, and military devices.[9−11] As a new type of free-space optical communication, the modulating retroreflector (MRR) communication technique used in the military field has attracted interest for use in the development of a transceiver with an electro-optic modulation function in the near-infrared range.[12−14] Because of the coexistence of near-infrared optical signal emission and detection capabilities in multiple quantum wells (MQWs), InP-based materials with AlInGaAs MQWs represent a promising material choice for the design of a transceiver with near-infrared electro-optic modulation characteristics.[15−17] The transceiver made of MQWs can significantly reduce the cost and size for terminal devices of optical communication and sensing networks. Because the transceiver made of MQWs has the potential to achieve multifunction of optical signal emitting/detection and modulation on an ultrasmall wafer with MQWs, it provides an approach to perform a variety of optoelectronic functions on a single terminal.

Some remarkable research into the electro-optic modulation characteristics of MQWs has been reported that focused on light source power modulators, optical switching, optical interconnections, and other on-chip optical applications.[18−20] Akie et al. proposed a tapered coupler-based electro-optic modulator composed of GeSn/SiGeSn MQWs on a Ge-on-Si platform for mid-infrared-integrated optical active device applications.[21] Sadiq et al. investigated the electro-optic properties of ramped asymmetric AlInGaAs MQWs for use in refractive index modulation.[22] Chaisakul et al. reported a high-speed Ge/SiGe MQW-based electroabsorption waveguide modulator for use in energy-efficient optical interconnections.[18] The previous work on the electro-optic modulation characteristics of MQWs mentioned above is mainly concerned with their applications as optical interconnections and optical switching devices in photonic chips in the infrared range.[18,19,21,22] The above impressive work makes an in-depth analysis of the mechanism of MQW electro-optic modulation and increases the operating frequency of the devices to GHz. As a comparison, this paper attempts to extend the electro-optic modulation range of AlInGaAs MQWs devices to a wider spectral range covering visible light and study the application potential of AlInGaAs MQWs devices as an independent transceiver in optical communication and sensing.

Based on the coexistence of luminescence and detection properties in MQWs, integrated photonic chips with a light

Received: July 21, 2021
Published: September 3, 2021

https://doi.org/10.1021/acsomega.1c03865
ACS Omega 2021, 6, 23614−23620

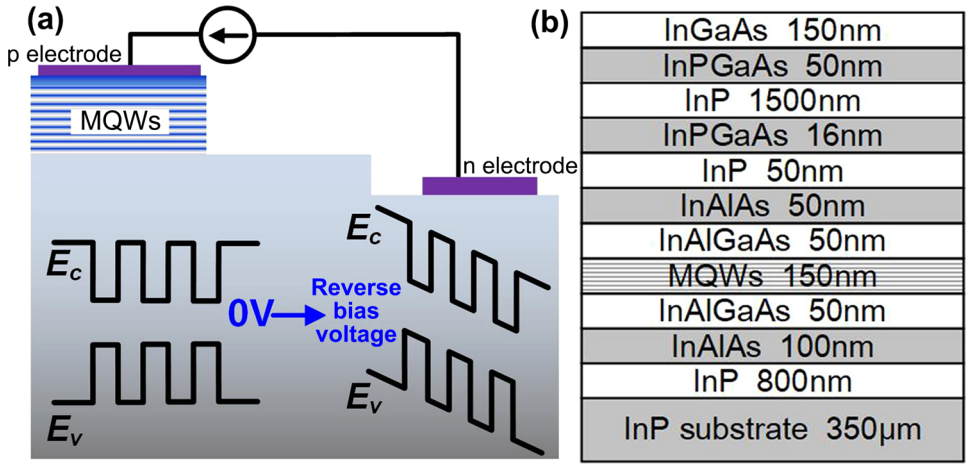

Figure 1. (a) Working mechanism of the AlInGaAs MQW transceiver with electro-optic modulation characteristics. (b) Cross section of the InP-based wafer structure with AlInGaAs MQWs.

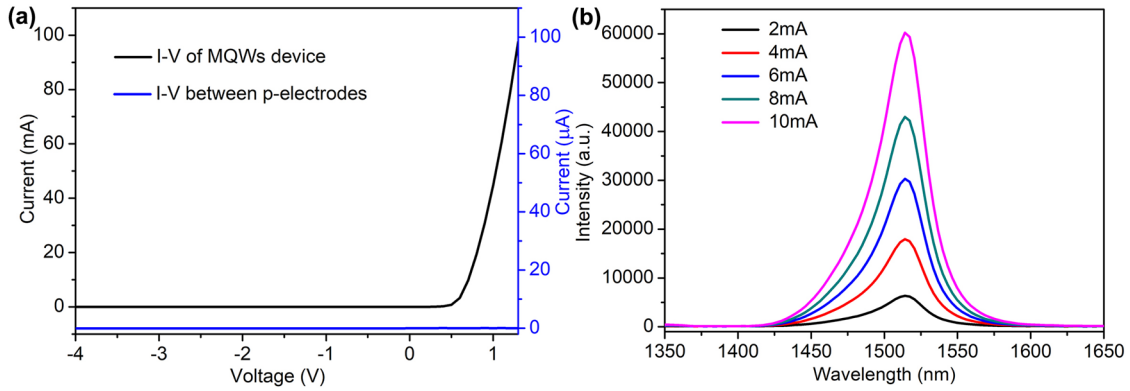

Figure 2. (a) Measured $I-V$ curves of the AlInGaAs MQW transceiver. (b) Electroluminescence characteristics of the AlInGaAs MQW transceiver.

source, a waveguide, and a photodetector have been realized on GaN-based wafers with MQWs for full-duplex communication in the visible range in our previous work.[23−26] We also proposed a monolithic photonic chip with multifunction light emission/detection and electro-optic modulation capabilities in the near-infrared range.[27] In this work, we further study an AlInGaAs MQW transceiver with electro-optic modulation characteristics for free-space optical communication and sensing applications over a broad spectral range. Two identical AlInGaAs MQW diodes are prepared to perform light emission/detection/modulation on a single wafer. The AlInGaAs MQW transceiver shows excellent electrical characteristics when acting as both the transmitter and receiver. The device also realizes a clear electro-optic modulation performance for broad-spectrum light. We perform an electro-optically modulated optical communication experiment using the designed transceiver for self-transmission and self-reception operations based on asymmetric optical links, and the transceiver is able to detect the modulation of the optical signal caused by environmental changes and electrical signals simultaneously.

The schematic in Figure 1a illustrates the working mechanism of the AlInGaAs MQW transceiver with electro-optic modulation characteristics. The most important part of the AlInGaAs MQW transceiver is the MQW structure with its different energy bands. The optical absorption of MQWs is affected by the electric field generated by the reverse bias voltage based on the quantum confinement Stark effect.[28] When the reverse bias voltage increases, the electronic state moves toward a lower energy and the hole state moves toward a higher energy under the built-in polarized electric field. The energy band of the MQWs is tilted, which leads to a change in the optical absorptivity. The energy movement caused by the built-in polarized electric field is given by eq 1.

$$\Delta E = -24\left(\frac{2}{3\pi}\right)^6 \frac{e^2F^2m_{tot}^*L^4}{\hbar^2} \quad (1)$$

Here, ΔE is the energy shift value, e is the electron quantity, F is the built-in electric field strength, m_{tot}^* is the effective mass of the carrier, L is the width of the quantum well, and $\hbar$ is the Planck constant. All of the parameters except the Planck constant belong to the characteristics of multiple quantum well materials, and the characteristics of multiple quantum well materials strongly affect the electro-optic modulation effect of the transceiver. The active area of the transceiver will also affect the electro-optic modulation effect. The larger the active area, the more light is collected and modulated. The AlInGaAs MQW transceiver is realized on a commercial InP-based wafer (Cengol Corporation, Beijing, China), as shown in Figure 1b. The substrate is composed of InP with a thickness of 350 μm. The epitaxial layer consists of ∼800-nm-thick InP, ∼100-nm-thick InAlAs, ∼50-nm-thick InAlGaAs, ∼150-nm-thick MQWs (five pairs of AlInGaAs MQWs), ∼50-nm-thick InAlGaAs, ∼50-nm-thick InAlAs, ∼50-nm-thick InP, ∼16-nm-thick

https://doi.org/10.1021/acsomega.1c03865
ACS Omega 2021, 6, 23614−23620

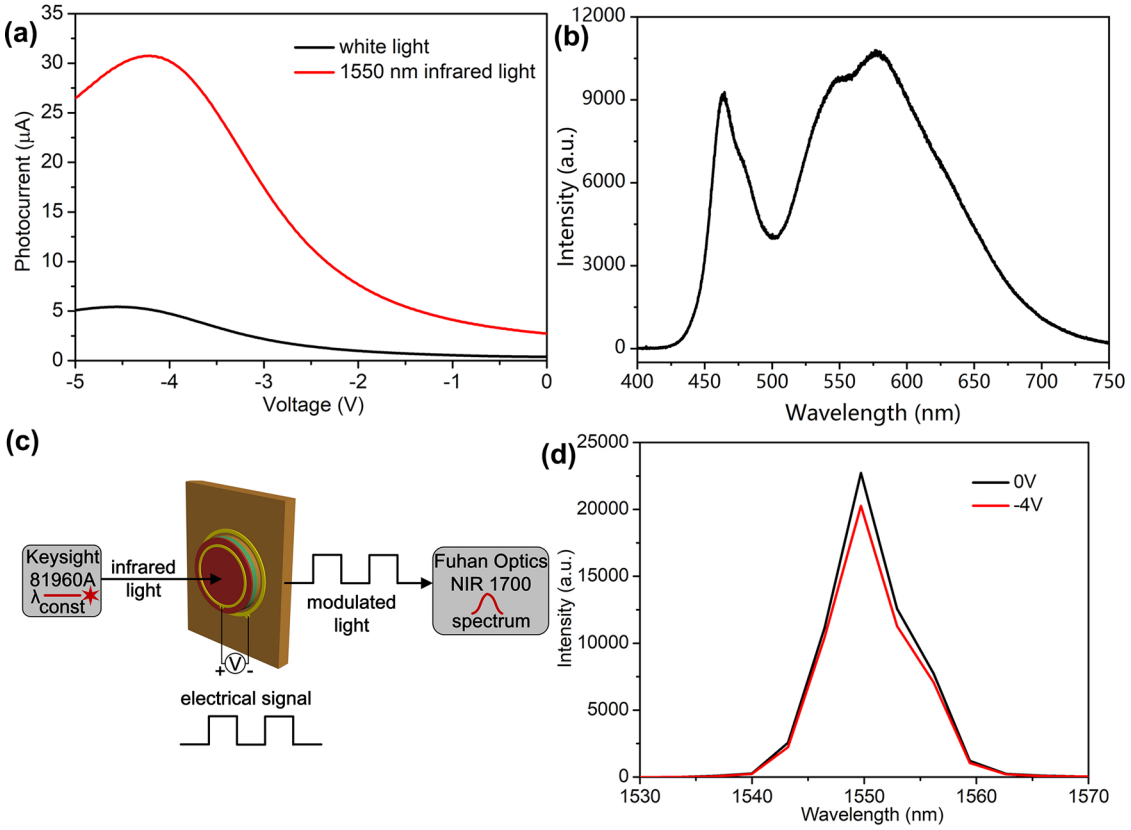

Figure 3. (a) Photocurrent characteristics of the AlInGaAs MQW transceiver as a function of reverse bias voltage. (b) Spectrum of a white light source. (c) Schematic illustration of the transmission electro-optic modulation test experimental setup. (d) Modulated spectra obtained for 1550 nm infrared light under different reverse bias voltages on the AlInGaAs MQW transceiver.

InPGaAs, ∼1500-nm-thick InP, ∼50-nm-thick InPGaAs, and ∼150-nm-thick InGaAs layers.

RESULTS AND DISCUSSION

The optoelectrical characteristics of the AlInGaAs MQW transceiver for light transmission are measured using a probe station connected to a semiconductor device parameter analyzer (Agilent, B1500A). Figure 2a shows the current−voltage (I−V) curves of the AlInGaAs MQW transceiver. The turn-on voltage is approximately 0.5 V. The current increases rapidly when the turn-on voltage is exceeded, and the current reaches 100 mA (i.e., the saturation value of the semiconductor device parameter analyzer) at a voltage of 1.3 V. The current between the p-electrodes of the two AlInGaAs MQW transceivers is approximately 0 μA. The two devices have been electrically isolated completely, and the devices thus work independently. The electroluminescence (EL) characteristics of the AlInGaAs MQW transceiver are measured using a collimating mirror and a near-infrared spectrometer (Fuhan Optics, NIR 1700) in the vertical direction, as shown in Figure 2b. A dominant EL peak is observed at 1514 nm. Because the current affects the light intensity, the peak light intensity at 10 mA is 9.48 times stronger than that at 2 mA. The device has excellent electrical characteristics, and the transmitted light intensity is strongly modulated by the current. These results demonstrate that the device is highly suitable for use as a transmitter in optical communications.

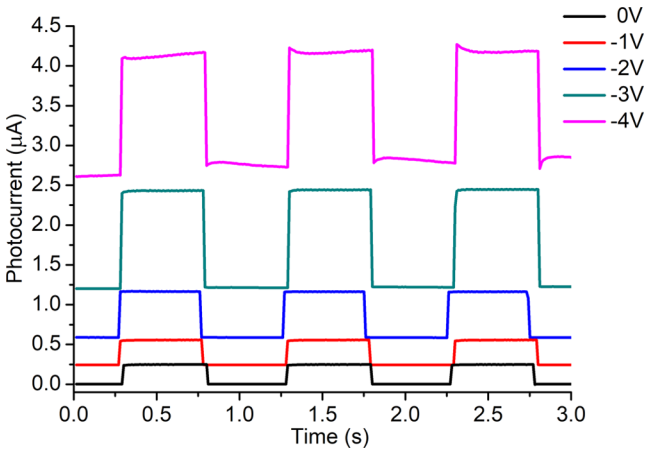

Figure 4. Photocurrent signals of the AlInGaAs MQW transceiver varying with square wave white light signals at 1 Hz under different reverse bias voltages.

Under the application of a negative voltage, the AlInGaAs MQW transceiver operates as a receiver, and its photocurrent is measured by irradiating the device using both white light and a 1550 nm infrared light source (Keysight, 81960A). There are two peaks in the white light spectrum in Figure 3b, which are 464 and 582 nm. As shown in Figure 3a, the photocurrent varies with the reverse bias voltage. When the reverse bias voltage increases from 4.55 to 0 V, the photocurrent obtained for white light decreases from 5.43 to 0.39 μA, and the modulation ratio is approximately 13.9. When the reverse bias voltage increases from 4.22 to 0 V, the photocurrent obtained for 1550 nm infrared light decreases from 30.8 to 2.73 μA, and the modulation ratio is approximately 11.3. The AlInGaAs

https://doi.org/10.1021/acsomega.1c03865
ACS Omega 2021, 6, 23614−23620

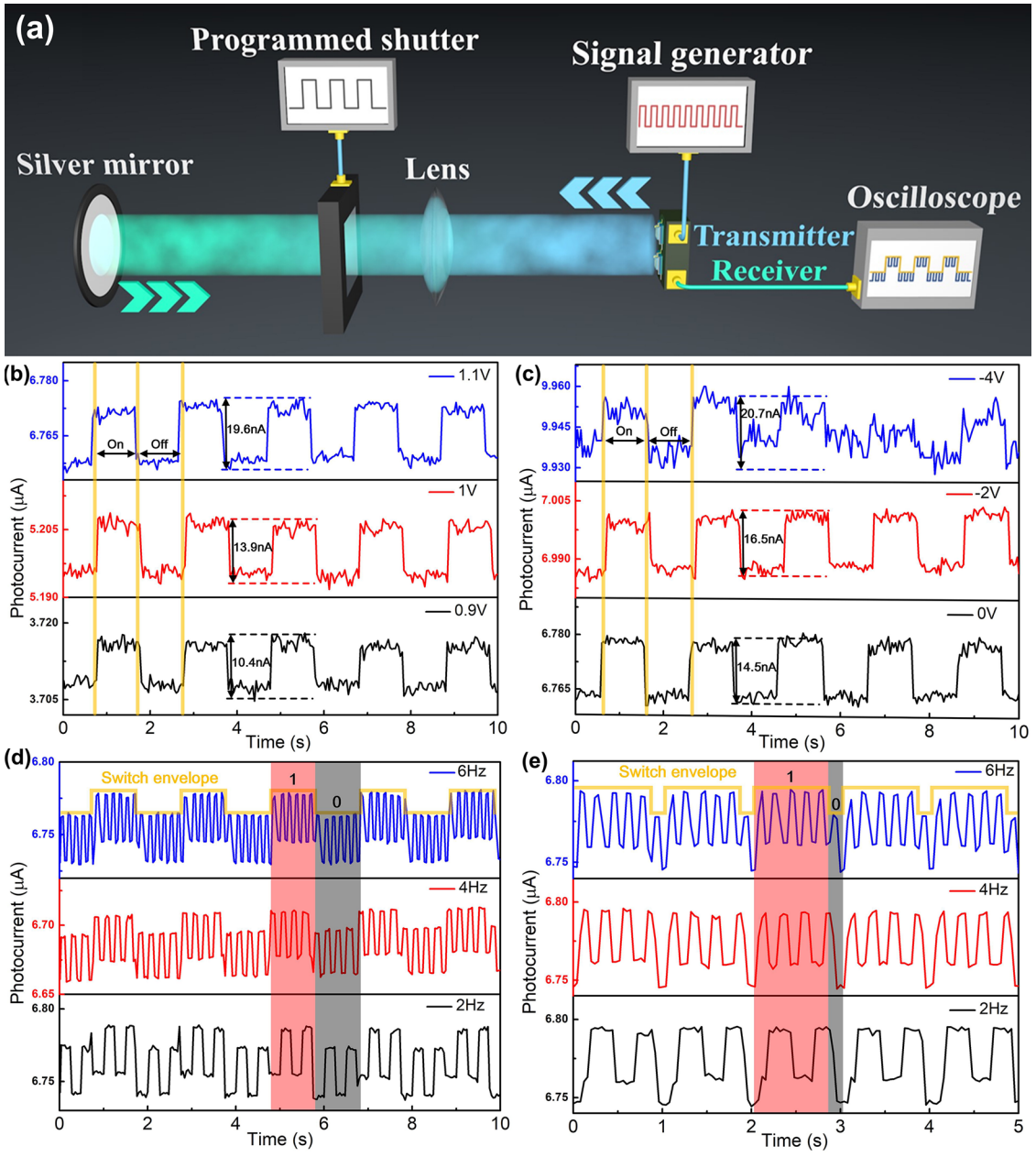

Figure 5. (a) Schematic of the experimental setup for electro-optically modulated optical communication with self-transmitting and self-receiving operations based on asymmetric optical links for the AlInGaAs MQW transceiver. (b) Variation of the receiver photocurrent with square wave forward voltage at 1 Hz applied to the transmitter under different forward voltages. (c) Variation of the receiver photocurrent with square wave forward voltage at 1 Hz applied to the transmitter under different reverse bias voltages. (d) Photocurrent superimposed signals for forward voltages at different frequencies and a 0.5 Hz mechanical shutter with a 0.5 duty cycle. (e) Photocurrent superimposed signals for forward voltages at different frequencies and a 1 Hz mechanical shutter with a 0.8 duty cycle.

MQW transceiver thus shows an obvious electro-optic modulation performance for broad-spectrum light. The absorption coefficient of 1550 nm infrared is larger than that of white light. The variation of the absorption coefficient of 1550 nm infrared is also greater caused by electro-optic modulation. We built a transmission test experiment setup to enable further characterization of the electro-optic modulation characteristics of the AlInGaAs MQW transceiver, as illustrated in Figure 3c, in which 1550 nm infrared light is coupled into the optical fiber and then irradiates the top surface of the transceiver in a normal incidence mode. The reverse bias voltage applied to the AlInGaAs MQW transceiver is controlled using an external dc power supply. Because the InP substrate is transparent to infrared light, the modulated light can be captured using an optical fiber with a transmission mode. Finally, the modulated light is coupled into the near-infrared spectrometer. As shown in Figure 3d, the peak intensity of the infrared light decreases from 22725 to 20257.8 au when the bias voltage is increased from 0 to 4 V. The modulation ratio of the 1550 nm light intensity is thus approximately 12.2%. The modulation effect when characterized using the light intensity is not as obvious as that obtained based on the photocurrent. This difference can be attributed to the fact that the spot size of the infrared light is larger than the active area of the transceiver, which means that

https://doi.org/10.1021/acsomega.1c03865
ACS Omega 2021, 6, 23614−23620

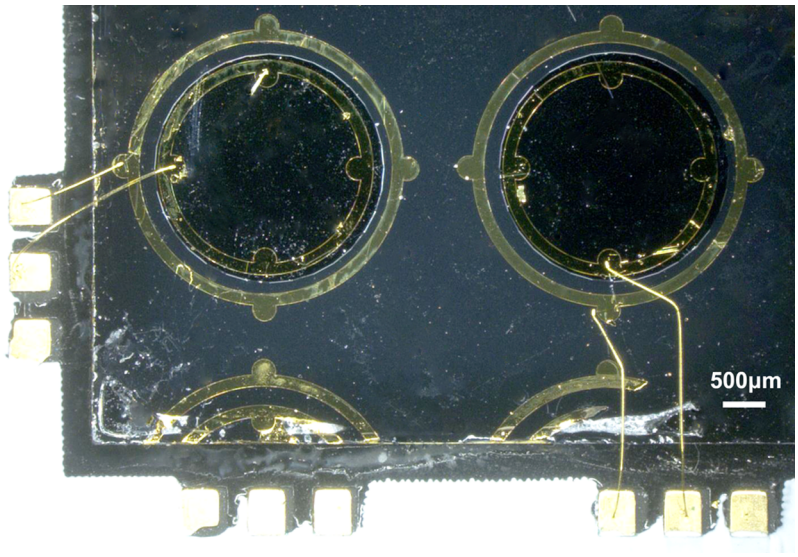

Figure 6. Optical microscope image of two AlInGaAs MQW transceivers.

most of the infrared light passes through the transceiver during the transmission test without being modulated.

To characterize the electro-optic modulation effect of the AlInGaAs MQW transceiver on white light, we illuminate the transceiver with a white light signal with a square wave pattern at 1 Hz and test its photocurrent. Figure 4 shows the variation of the photocurrent of the AlInGaAs MQW transceiver with the optical signal at 1 Hz at different reverse bias voltages. The photocurrent of the AlInGaAs MQW transceiver is also a square wave signal at 1 Hz and shows a good response to the square wave white light signal. The photocurrent at higher values of the square waves increases from 0.24 to 4.22 μA when the bias voltage increases from 0 to 4 V. The photocurrent modulation ratio for the high and low values of the square wave signal decreases from 97.6 to 1.55 when the bias voltage increases from 0 to 4 V. Although the photocurrent is higher at 4 V for the amplitude modulated optical communication signal, the device shows better modulation characteristics at 0 V.

Finally, we performed the electro-optically modulated optical communication experiment with self-transmitting and self-receiving operations based on asymmetric optical links for the AlInGaAs MQW transceiver, as shown in Figure 5a. The two transceivers work separately as a transmitter and a receiver. We load the electrical signal onto the transmitter, and the electrical signal is then converted into an optical signal in the infrared range. The infrared light emitted by the transmitter reaches the silver mirror. This infrared light is then reflected back and is captured by the receiver and converted from an optical signal into a photocurrent. The mechanical shutter also modulates the reflected light. The infrared light is modulated by both the electrical signal and the mechanical shutter in the asymmetric optical links and thus forms the superimposed signal. Figure 5b shows the results obtained when the receiver is operated at a reverse bias voltage of 0 V, and forward voltages from 0.9 to 1.1 V are applied to the transmitter. The infrared light is modulated by the mechanical shutter at 0.5 Hz. The modulation amplitude of the photocurrent is enhanced from 10.4 to 19.6 nA. Figure 5c shows the results obtained when the transmitter operates at a forward voltage of 1 V and reverse bias voltages from 0 to 4 V are applied to the receiver. The modulation by the mechanical shutter is the same as that used in the case of Figure 5. The modulation amplitude of the photocurrent is increased from 14.5 to 20.7 nA. However, when the reverse bias voltage decreases, the modulation waveform of the photocurrent becomes unstable. These results demonstrate that these transceivers can be used with appropriate electrical parameters to emit and receive modulated light and thus detect environmental changes in the form of the operation of the mechanical shutter. A forward voltage (square wave with peak-to-peak voltage Vpp of 1 mV and offset voltage Voffset of 1 V) at different frequencies (2−6 Hz) is then applied to the transmitter. The frequency of mechanical shutter operation is 0.5 Hz, and the duty cycle is 0.5. The superimposed optical signal modulated by both the forward voltage and the mechanical shutter is then captured by the receiver and converted into a photocurrent, with results as shown in Figure 5d. In the results shown in Figure 5e, the forward voltage parameters remain unchanged. The mechanical shutter frequency increases to 1 Hz and the duty cycle is 0.8. These results demonstrate that the AlInGaAs MQW transceiver is able to detect the modulation of the external optical signal by environmental changes while also transmitting modulated light. Additionally, the transceiver can identify both the environmental changes and the electrical signal from the same beam of reflected light.

CONCLUSIONS

A transceiver with electro-optic modulation characteristics for optical communication and sensing applications is realized on an InP-based wafer with AlInGaAs MQWs. The energy band of the MQWs is tilted by varying the bias voltage applied to the transceiver, which leads to the device's electro-optic modulation characteristics. When the transceiver operates as a transmitter, a dominant electroluminescence peak is observed at 1514 nm, and the peak light intensity at 10 mA is 9.48 times stronger than the peak observed at 2 mA. The transmitted light intensity is modulated strongly by the current. When the transceiver operates as a receiver, it shows obvious electro-optic modulation characteristics for broad-spectrum light. The photocurrent modulation ratios are 13.9 and 11.3 for white light and 1550 nm infrared light, respectively, with varying

https://doi.org/10.1021/acsomega.1c03865
ACS Omega 2021, 6, 23614−23620

reverse bias voltages. The modulated spectrum for 1550 nm light indicates that the modulation ratio of the light intensity is approximately 12.2% in the transmission mode. Finally, we performed an electro-optically modulated optical communication experiment with self-transmitting and self-receiving operations based on the use of asymmetric optical links for the transceiver. The transceiver identifies both environmental changes and forward electrical signals with different frequencies in the form of superimposed signals. This work provides a promising approach for the development of transceivers for use in optical modulating retroreflector (MRR) communication, environmental sensing, movement monitoring, and other applications.

EXPERIMENTAL SECTION

The fabrication process of the transceiver is described below. The mesa regions are patterned by photolithography and are then transferred to the InP-based wafer via inductively coupled plasma (ICP) etching for III−V materials to expose the N-type layer. Then, p/n electrodes with Ti (50 nm)/Pt (50 nm)/Au (400 nm) structures are formed by electron beam evaporation and lift-off processes. Figure 6 shows an optical microscope image of two AlInGaAs MQW devices. Two identical AlInGaAs MQW devices are prepared for light emission/detection/modulation operations. The active area of the AlInGaAs MQW transceiver is a circular region with a diameter of 6 mm. The p/n electrodes are shaped using 150-μm-wide rings with four pads. The devices are connected to a printed circuit board via lead wires on the pads.

AUTHOR INFORMATION

Corresponding Authors

Xin Li − *Grünberg Research Centre, Nanjing University of Posts and Telecommunications, Nanjing 210003, China; Key Lab of Broadband Wireless Communication and Sensor Network Technology (Nanjing University of Posts and Telecommunications), Ministry of Education, Nanjing 210003, China;* orcid.org/0000-0002-3370-013X; Email: lixin1984@njupt.edu.cn

Yongjin Wang − *Grünberg Research Centre, Nanjing University of Posts and Telecommunications, Nanjing 210003, China*; Email: wangyj@njupt.edu.cn

Authors

Xu Wang − *Grünberg Research Centre, Nanjing University of Posts and Telecommunications, Nanjing 210003, China*

Yun Li − *Grünberg Research Centre, Nanjing University of Posts and Telecommunications, Nanjing 210003, China*

Feifei Qin − *Grünberg Research Centre, Nanjing University of Posts and Telecommunications, Nanjing 210003, China*

Yan Jiang − *Grünberg Research Centre, Nanjing University of Posts and Telecommunications, Nanjing 210003, China*

Linning Wang − *Grünberg Research Centre, Nanjing University of Posts and Telecommunications, Nanjing 210003, China*

Complete contact information is available at: https://pubs.acs.org/10.1021/acsomega.1c03865

Author Contributions

The manuscript was written through the contributions of all authors. All authors have given approval to the final version of the manuscript.

Notes

The authors declare no competing financial interest.

ACKNOWLEDGMENTS

This work was jointly supported by the China Postdoctoral Science Foundation (2018M640508), 1311 Talent Program of Nanjing University of Posts and Telecommunications, the open research fund of Key Lab of Broadband Wireless Communication and Sensor Network Technology (Nanjing University of Posts and Telecommunications), Ministry of Education, the National Natural Science Foundation of China (61904086, 62005130), and the Natural Science Foundation of Jiangsu Province (BK20190726, BK20200755, BK20170909). The authors thank David MacDonald, M.Sc., from Liwen Bianji, Edanz Editing China (www.liwenbianji.cn/ac), for editing the English text of a draft of this manuscript.

REFERENCES

(1) Shang, T.; Jia, J.; Wang, X. Analysis and design of a multi-transceiver optical cylinder antenna for mobile free space optical communication. *Opt. Laser Technol.* **2012**, *44*, 2384−2392.

(2) Mai, V. V.; Kim, H. In *Wide Field-of-view Transceiver Design for Bidirectional Free-space Optical Communication Systems*, Optoelectronics and Communications Conference (OECC), 2019; pp 1−3.

(3) Abou-Rjeily, C.; Slim, A. Cooperative diversity for free-space optical communications: transceiver design and performance analysis. *IEEE Trans. Commun.* **2011**, *59*, 658−663.

(4) Shinagawa, M.; Fukumoto, M.; Ochiai, K.; Kyuragi, H. A near-field-sensing transceiver for intrabody communication based on the electrooptic effect. *IEEE Trans. Instrum. Meas.* **2004**, *53*, 1533−1538.

(5) Khalid, A.; Asif, H. M.; Mumtaz, S.; Al Otaibi, S.; Konstantin, K. Design of MIMO-visible light communication transceiver using maximum rank distance codes. *IEEE Access* **2019**, *7*, 89128−89140.

(6) Nakhkoob, B.; Bilgi, M.; Yuksel, M.; Hella, M. Multi-transceiver optical wireless spherical structures for MANETs. *IEEE J. Sel. Areas Commun.* **2009**, *27*, 1612−1622.

(7) Altabas, J. A.; Izquierdo, D.; Lazaro, J. A.; Garces, I. Chirp-based direct phase modulation of VCSELs for cost-effective transceivers. *Opt. Lett.* **2017**, *42*, 583.

(8) Lee, T. H.; Oh, S. H.; Kim, P. J.; Han, Y.-G.; Kim, C.-S.; Jeong, M. Y. Imprinted bidirectional waveguide platform for large-core optical transceiver. *Opt. Lett.* **2011**, *36*, 2324.

(9) Nasr, I.; Jungmaier, R.; Baheti, A.; Noppeney, D.; Bal, J. S.; Wojnowski, M.; Karagozler, E.; Raja, H.; Lien, J.; Poupyrev, I.; Trotta, S. A highly integrated 60 GHz 6-channel transceiver with antenna in package for smart sensing and short-range communications. *IEEE J. Solid-State Circuits* **2016**, *51*, 2066−2076.

(10) Onibonoje, M. O.; Nwulu, N. I.; Bokoro, P. N. In *An Internet-of-things Design Approach to Real-time Monitoring and Protection of a Residential Power System*, IEEE 7th International Conference on Smart Energy Grid Engineering (SEGE), 2019; pp 113−119.

(11) Dano, E. B. In *A Case Study on the Architectural Development of a Transceiver Assembly*, International Symposium on Systems Engineering (ISSE), 2019; pp 1−6.

(12) Goetz, P. G.; Rabinovich, W. S.; Gilbreath, G. C.; Mahon, R.; Ferraro, M. S.; Swingen, L.; Walters, R. J.; Messenger, S. R.; Wasiczko, L. M.; Murphy, J.; Creamer, N. G.; Burris, H. R.; Stell, M. F.; Moore, C. I.; Binari, S. C.; Katzer, D. S. In *Multiple Quantum well Based Modulating Retroreflectors for Inter- and Intra-spacecraft Communication*, Conference on Photonics for Space Environments XI, 2006; 63080A.

(13) Goetz, P. G.; Rabinovich, W. S.; Mahon, R.; Murphy, J. L.; Ferraro, M. S.; Suite, M. R.; Smith, W. R.; Xu, B. B.; Burris, H. R.; Moore, C. I.; Schultz, W. W.; Mathieu, B. M.; Hacker, K.; Reese, S.; Freeman, W. T.; Frawley, S.; Colbert, M. In *Modulating Retro-reflector Lasercom Systems at the Naval Research Laboratory*, Military Communications Conference, 2010; pp 1601−1606.

(14) Manning, S.; Mudge, K.; Grant, K.; Clare, B.; Arnold, J. P.; Biggs, C.; Cowley, W. G. In *Long-range Modulating Retroreflector Communications*, IEEE International Conference on Space Optical Systems and Applications (ICSOS), 2017; pp 233−239.
(15) Mura, E. E.; Gocalinska, A. M.; O'Brien, M.; Loi, R.; Juska, G.; Moroni, S. T.; O'Callaghan, J.; Arredondo, M.; Corbett, B.; Pelucchi, E. Importance of overcoming MOVPE surface evolution instabilities for>1.3 μm metamorphic lasers on GaAs. *Cryst. Growth Des.* **2021**, *21*, 2068−2075.
(16) Sibirmovsky, Y. D.; Kargin, N. I.; Vasil'evskii, I. S. In *Modelling of Quantum-confined Stark Effect in III-V Heterostructures for Electro-optic Modulator Applications*, PhotonIcs & Electromagnetics Research Symposium - Spring (PIERS-Spring), 2019; pp 733−740.
(17) Abbasi, A.; Verbist, J.; Shiramin, L. A.; Verplaetse, M.; De Keulenaer, T.; Vaernewyck, R.; Pierco, R.; Vyncke, A.; Yin, X.; Torfs, G.; Morthier, G.; Bauwelinck, J.; Roelkens, G. 100-Gb/s electro-absorptive duobinary modulation of an InP-on-Si DFB laser. *IEEE Photonics Technol. Lett.* **2018**, *30*, 1095−1098.
(18) Chaisakul, P.; Marris-Morini, D.; Rouifed, M.-S.; Isella, G.; Chrastina, D.; Frigerio, J.; Le Roux, X.; Edmond, S.; Coudevylle, J.-R.; Vivien, L. 23 GHz Ge/SiGe multiple quantum well electro-absorption modulator. *Opt. Express* **2012**, *20*, 3219.
(19) Wu, P. C.; Pala, R. A.; Kafaie Shirmanesh, G.; Cheng, W.-H.; Sokhoyan, R.; Grajower, M.; Alam, M. Z.; Lee, D.; Atwater, H. A. Dynamic beam steering with all-dielectric electro-optic III−V multiple-quantum-well metasurfaces. *Nat. Commun.* **2019**, *10*, No. 3654.
(20) Adnan, M.; Rao, K. N.; Acharyya, J. N.; Kumar, D.; Dehury, K. M.; Prakash, G. V. Synthesis, structural, linear, and nonlinear optical studies of inorganic−organic hybrid semiconductors (R−C 6 H 4 CHCH 3 NH 3) 2 PbI 4, (R = CH 3, Cl). *ACS Omega* **2019**, *4*, 19565−19572.
(21) Akie, M.; Fujisawa, T.; Sato, T.; Arai, M.; Saitoh, K. GeSn/SiGeSn multiple-quantum-well electroabsorption modulator with taper coupler for mid-infrared Ge-on-Si platform. *IEEE J. Sel. Top. Quantum Electron.* **2018**, *24*, 1−8.
(22) Sadiq, M. U.; O'Callaghan, J.; Roycroft, B.; Thomas, K.; Pelucchi, E.; Peters, F. H.; Corbett, B. Study of electro-optic effect in asymmetrically ramped AlInGaAs multiple quantum well structures. *Phys. Status Solidi A* **2016**, *213*, 930−935.
(23) Li, X.; Jiang, Y.; Li, J.; Shi, Z.; Zhu, G.; Wang, Y. Integrated photonics chip with InGaN/GaN light-emitting diode and bended waveguide for visible-light communications. *Opt. Laser Technol.* **2019**, *114*, 103−109.
(24) Wang, Y.; Wang, X.; Zhu, B.; Shi, Z.; Yuan, J.; Gao, X.; Liu, Y.; Sun, X.; Li, D.; Amano, H. Full-duplex light communication with a monolithic multicomponent system. *Light Sci. Appl.* **2018**, *7*, No. 83.
(25) Wang, Y.; Wang, X.; Yuan, J.; Gao, X.; Zhu, B. Monolithic III-nitride photonic circuit towards on-chip optical interconnection. *Appl. Phys. Express* **2018**, *11*, No. 122201.
(26) Wang, L.; Li, X.; Gao, X.; Jia, B.; Guan, Q.; Ye, Z.; Fu, K.; Jin, R.; Wang, Y. Asymmetric optical links using monolithic III-nitride diodes. *Opt. Lett.* **2021**, *46*, 376−379.
(27) Li, X.; Ni, S.; Jiang, Y.; Li, J.; Wang, W.; Yuan, J.; Li, D.; Sun, X.; Wang, Y. AlInGaAs multiple quantum well-integrated device with multifunction light emission/detection and electro-optic modulation in the near-infrared range. *ACS Omega* **2021**, *6*, 8687−8692.
(28) Bar-Joseph, I.; Klingshirn, C.; Miller, D. A. B.; Chemla, D. S.; Koren, U.; Miller, B. I. Quantum-confined stark effect in InGaAs/InP quantum wells grown by organometallic vapor phase epitaxy. *Appl. Phys. Lett.* **1987**, *50*, 1010−1012.

https://doi.org/10.1021/acsomega.1c03865
ACS Omega 2021, 6, 23614−23620